IN-ORBIT CHECKOUT OF THE IRAS GYROSCOPES

J.F.M. van Casteren

Fokker B.V.
Space Division
Schiphol-Oost
The Netherlands

ABSTRACT

After a description of the IRAS gyroscope package, those gyro characteristics which are of specific importance from the mission operations point of view, will be addressed. It will be discussed which of those characteristics can be determined to sufficient accuracy pre-launch and which ones will change in the launch environment and consequently have to be re-determined during the in-orbit checkout. The expected in-orbit stability of the considered characteristics and the required accuracy dictates the frequency of special flight sequences throughout the routine phase to assist in verification and maintenance of the gyro performance. The effects of special phenomena as pivot clearance, scalefactor dependency on temperature and scalefactor and drift dependency on clockfrequency, will be comtemplated. Finally the in-flight test method and ground evaluation method are described.

Keywords: In-orbit checkout: gyroscopes; attitude control; Infra-Red Astronomical Satellite.

1. INTRODUCTION

The Infra-Red Astronomical Satellite, IRAS, scheduled for launch in August 1982, is a joint programme of the Netherlands, the United States and the United Kingdom. The satellite configuration is shown in figures 1 and 2. The mission objective is the completion of an all sky survey in the infrared wavelengths from 8 to 120 microns, and to observe infrared sources of special interest in more detail. The telescope will be cooled with super-fluid helium, contained in a dewar which surrounds the telescope. A description of the satellite and the mission design is given in refs. 1 and 2.

The selected orbit, see figure 3, is a 900 km sunsynchronous twilight orbit with an inclination of 99 degrees. The systematic sky survey will be performed such that the telescope scans around the earth-sun line (sunvector), pointing radially outwards from the earth with an allowable pitch angle of 30 degrees; the angle between the telescope boresight and the sunvector can be varied between 60 and 120 degrees.

The IRAS is a three axis stabilized satellite with a 2 Hz sampled data system for the attitude control sensors, controlled by a redundant on-board computer. The downlink frequency of attitude sensor outputs is 1 Hz. The tasks of the Attitude Control System (ACS), a responsibility of Fokker, are among other things:

- attitude safeguarding of the telescope against excessive heat input from the sun and the earth,
- control of the telescope towards the desired locations on the sky with an accuracy of 20 arcseconds,
- provision of sufficient data to the grounddata systems for reconstruction of the boresight attitude with an accuracy better than 20 arcseconds.

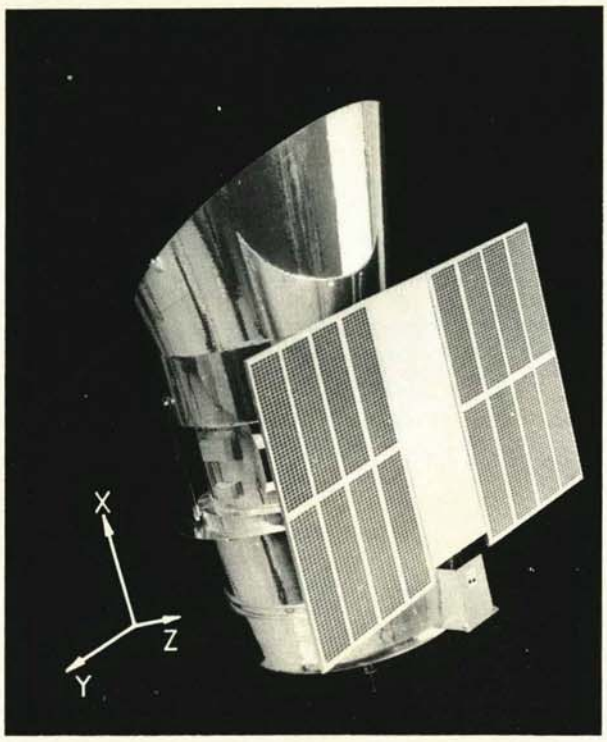

Figure 1. The Infra-Red Astronomical Satellite (front)

Proc. Int. Symp. Spacecraft Flight Dynamics, Darmstadt, FRG, 18-22 May 1981 (ESA SP-160, Aug. 1981)

Figure 2. The Infra-Red Astronomical Satellite (rear)

The ACS, (ref. 3), incorporates a partly redundant sensor configuration, providing several backup possibilities in case of failures in hardware or software. The mission critical processing functions house in a read only memory. A random access memory contains among other things the fine control algorithms and is reprogrammable from the ground. As prime actuators a set of three reaction wheels is used.

The satellite attitude is defined by the angle between the sunvector and the boresight (solar aspect angle θ) and by the angle about the sunvector ψ (see figure 4). This attitude is measured using a two axis Fine Sun Sensor (FSS) and a rate integrating Z-axis gyro (GYRZ). A two axis Star Sensor (SSE) of the slit type is employed to calibrate the telescope attitude. The X and Y axis gyros have been added to the gyro package to improve the satellite safety during eclipses and to allow observations to continue during the eclipse periods.

2. GYRO DESCRIPTION

The IRAS gyro package (ferranti type 125) consists of two units, namely the gyro sensor and the electronics unit. The gyro sensor contains four gyros designated as GYRX, GYRY, GYRZA, GYRZB, the Z-gyro being redundant. Each one is a single degree of freedom rate integrating gyroscope. Figure 5 shows the positions of these gyroscopes on the gyro frame and indicates the positive directions of their input, output and spin axes.

Also contained in the gyro sensor is the circuitry for thermal control of the gyro (70 $\pm$ 1°C) and an optical cube to enable correct alignment of the gyro axes at integration. The gyro electronics contains circuitry for running the gyros and for processing the gyro signals. It also contains an interface for transmitting data to the satellite on-board computer and power supply for powering the circuitry in the sensor and electronics. Each sensor will measure angular rates about its input axis and outputs a 16 bit word in the form of angular increments during 0.5 second intervals with a resolution of one arcsecond. Table 1 shows some typical gyro characteristics.

Maximum drift rate	1.5°/hr
Bias drift change after 2 weeks	<6"/hr
Random drift change over 30 min.	<3.6"/hr
Non-linearity	<0.02%
Long term scalefactor change	<0.004%/month
Short term scalefactor change	<0.002%/30 min

Table 1. Gyro characteristics

3. MISSION IMPORTANT GYRO CHARACTERISTICS

For each satellite axis one gyro is used to control and reconstruct the satellite attitude, making the gyro package a prime sensor for the mission. Evidently, the gyro output has to be related to the rate about the relevant satellite axis at any given time. For control purposes the stability of the transfer function is such that it is justifiable to assume it constant over a two weeks period.
For reconstruction purposes a Kalman filter technique is employed, re-estimating each second among other things the transfer function parameters of the three gyros.

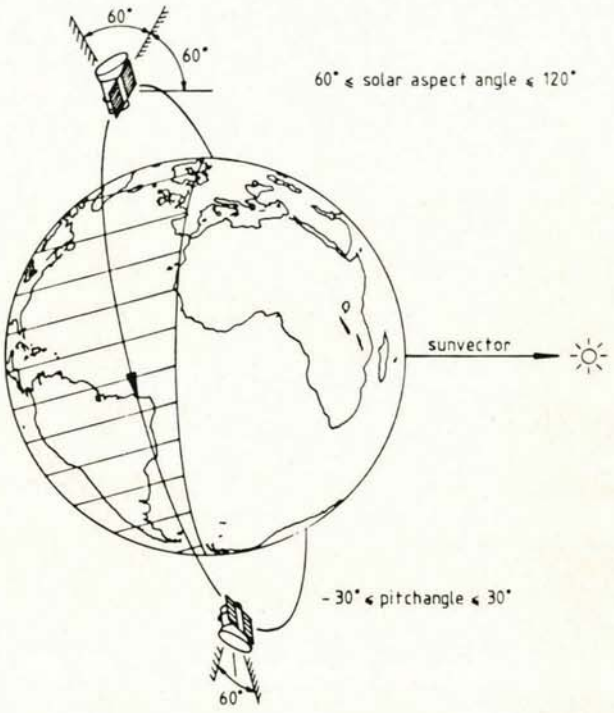

Figure 3. IRAS orbit geometry

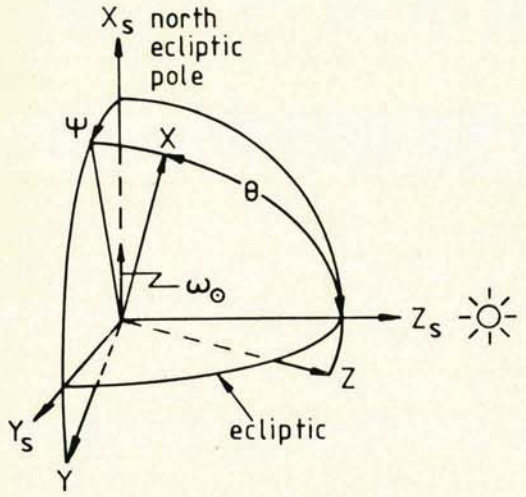

Ψ = angle about sunvector
θ = solar aspect angle
X Y Z = control coordinate frame
X_S Y_S Z_S = sun referenced frame

Figure 4. Definition of the IRAS attitude control frame

For the sake of description, let's concentrate now on the GYRZ, bearing in mind that the following considerations also apply to the other gyros. Starting with an attitude calibration with the SSE, (where the attitude found by the gyro is updated by the attitude as measured by the SSE) attitude errors around the sunvector will build up, due to the errors in the gyro transfer function, until the next attitude update where the control accuracy again instantly improves to the SSE accuracy.
At reconstruction only linearly developing errors in between SSE attitude calibrations will be eliminated due to the used reconstruction method. Consequently, gyro characteristics which cause slowly varying or constant gyro output errors do not affect the boresight position reconstruction accuracy.

The typical time between attitude calibrations is 30 minutes, so short term non-linear transfer function variations with a time constant less than this figure will not easily be filtered out at reconstruction. It is not appropriate to determine those characteristics in orbit; however, the mission requires that special attention be given to the design, development and manufacturing of the gyros to improve short term stability effects. In addition it is important that accuracy values of these characteristics be known pre-launch in order to make an accuracy analysis and to optimise the reconstruction algorithms.
Gyro parameters, which are used during the mission operations, must be established, i.e. characteristics that on the one hand are used as parameters in the on-board software and ground operations scheduling software to satisfy control accuracy requirements and on the other hand by the attitude reconstruction software to meet the stringent requirements on position accuracy of observed sources which ultimately appear in the infrared catalog.

Many error sources contribute to the gyro sensor output; the principal one for the rate integrating gyro is the drift rate instability.
The known systematic errors of drift, scale factor and input axis misalignment are corrected for in both the on-board software and the ground reconstruction software. Drift instability caused by thermal effects is minimized by automatically controlled heaters. Drift may be caused by torques exerted by spin motor power wires, bearing noise, changes in magnetic environment and spacecraft voltage fluctuations. The following characteristics and errors due to gyro imperfections, essential for mission operations, are considered:

- transfer function
  - drift, bias and random
  - scale factor
    - non-linearity
    - temperature effect
    - clockfrequency effect
- pivot clearance
- misalignment

These characteristics will be discussed in the following sections.

3.1. Drift

Bias drift is due to an error torque which is exerted by the elastic flexible leads carrying power to the spin motor. To a great extent this drift is fixed and can be compensated for, but some random changes preclude this solution.
For this reason drift is divided into two classes: fixed and random. Because of g-effects, earth rotation and temperature effects on earth, the drift will be determined in orbit. After determination and correction in flight, an uncertainty in bias drift stability of 12 "/hr per month remains. The drift will be determined and updated once a fortnight and is assumed to change linearly in time. Thus a maximum of 6 "/hr uncertainty remains. Note that for the mission the "effective bias drift error" is important. This may be defined as the error with which the bias drift is determined in flight and the bias drift change thereafter until the moment of redetermination and update. The phenomena that cause random drift are thermal instability, fluid density changes, bearing noise and the like. Random drift may be characterised as a short term random walk and cannot be corrected for although it may have a significant effect. The maximum deviation from the average bias drift during a 30 minute period is 3.6 "/hr.

3.2. Scale factor

Gyro scale factor errors are of particular importance to slews and scans. Nominally the scalefactor value equals one, i.e. one count in the gyro output resembles one arcsec rotation about the input axis. As with the other gyro parameters it is difficult to measure the scale factor accurately enough under earth conditions. Moreover the scalefactor will change under influence of the launch environment, resulting in a scalefactor uncertainty once in flight of 0.2%. After calibration these errors will be eliminated, however the following uncertainties remain:

- SF stability better than 0.004%/month

- SF short term deviation within 30 minutes 0.002% and maximum deviation between two successive 30 minutes periods: 0.002%.
- SF non-linearity will remain less than 0.02% in a best fit curve error band.

Gyro related scalefactor changes necessitate a scalefactor re-determination once every 2 weeks.

Whereas the gyroscope sensor is very well temperature controlled, the gyro electronics is not. The change in scalefactor per Kelvin has been measured to be 0.0025% per 2 K.
This 2 K corresponds to the maximum expected gyro electronics temperature change during a two weeks period. The resulting deviation of the scalefactor with respect to the values used in the on-board software leads to a small error angle at control during scans and slews.
The pointings itself will not be affected.

The gyro scalefactor depends directly upon the frequency of the satellite clock.

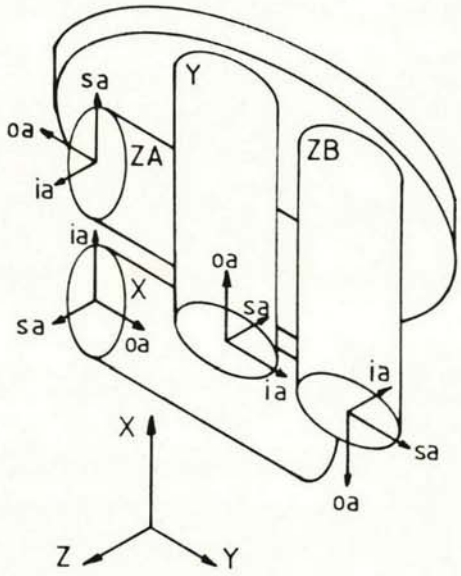

Figure 5. Gyropackage

This is due to the fact that both the gyro rotor frequency and the pulse length are based on the clockfrequency.
A one ppm clockfrequency increase results in a decrease of the scalefactor with one ppm and a decrease of the drift with two ppm.
Although the effects on the scalefactor of clock-frequency and gyro electronics temperature changes are automatically compensated once every 2 weeks, these changes will be monitored carefully by spacecraft engineers.

3.3. Pivot clearance

Due to the mechanical clearances in the gyro float pivots, the float can rotate through a small angle about the gyro input axis, as shown in figure 6. Under steady state conditions the float will adapt a preferred position and pivot clearance effects will not be evident. However, if the gyro is rotated about its output axis the float will rotate about its inputs axis until movement is restricted by the pivots. If rotation about the output axis is reversed the float will rotate about the input axis in opposite direction across the pivot clearance until it is again restricted by the pivots.
The rotation of the float will directly be measured by the sensor and be reflected in the output. For the employed gyro the freedom of rotation of the float about the input axis is smaller than 14 arcsec from end to end. The transition rate of the float is dependent on the applied rate about the output axis and is approximately one percent of the latter rate. For output axis rates of less than 1.5 arcsec/sec the float transition rate equals a constant 0.015 arcsec/sec. The maximum transition time amounts to 15.6 minutes.

Figure 5 shows that the output axes of all gyros are aligned with either the satellite X- or Y-axis.

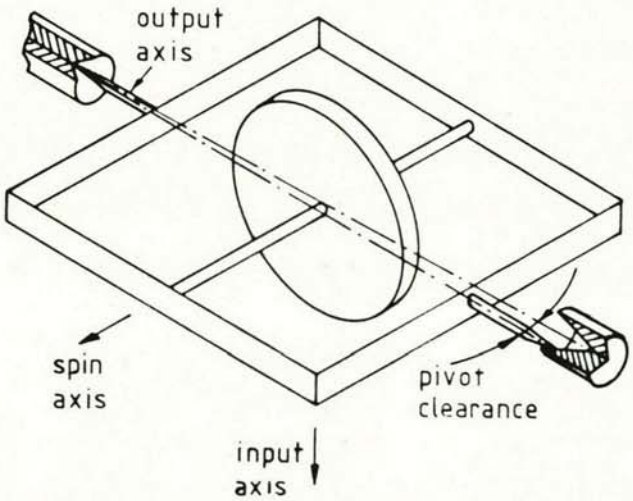

Figure 6. Gyro pivot clearance

During observation scans and pointings the satellite will limit cycle about these axes with a maximum velocity of 5 arcsec/sec and a period of 5 seconds. With reference to the transition rates mentioned above it is concluded that the pivots will either limit cycle about some preferred position with an amplitude of a fraction of an arcsecond or that the pivots will continuously be limited by the pivot restriction. During these steady states pivot clearance effects will not be noticeable. However, during a slew from one observation to the next, generally rates will occur about both the satellite X- and Y-axes causing the pivots of the gyros to transit to a restriction rapidly. During the following observation a slow transition of the pivot to a preferred state or to the other restriction may occur, causing a gyro output error.

Throughout the routine phase the pivot clearance effects will not be taken into account at observation planning. Pending a currently on-going investigation it may be corrected for at reconstruction.

3.4 Misalignment

A misalignment between the gyro input axis and the axes of the telescope will exist. Using the SSE, which is located in the focal plane of the telescope, these misalignments can be determined. Misalignment changes during the mission will mainly be caused by thermal changes. The most significant thermal changes originate from changes in solar aspect angle, which results in misalignment changes about the satellite Y-axis.

Obviously gyro input axis misalignment is something to take into account for a high accuracy astronomy mission. The onboard software contains a provision (refer to section 4) to correct the measured angular increments about the gyro input axes for misalignments to obtain the angular increments about the control coordinate frame axes. (see figure 4). After integration of the gyro package the misalignments are measured. In the launch environment the gyro misalignment is expected to change in the order of an arcminute. Therefore the misalignments will be determined during in orbit checkout. The misalignment stability dictates a verification once every 2 weeks.

4. GYRO ON-BOARD SOFTWARE

The ACS uses a control coordinate frame. Gyro sensor outputs have to be translated into angular increments about the axes of this control frame. This is established on-board by the transfer functions and a misalignment correction.

The gyro transfer function is defined as the relation between the angular increment per half second about the gyro input axis w.r.t. an inertial frame and the gyro output per half second. These transfer functions (refer figure 7) are approximated in the on-board software by the following expression:

$$\vec{\Delta\varphi}_{G_i} = \vec{N} * \vec{SF} + \vec{D} \qquad (1)$$

where:

$\vec{\Delta\varphi}_{G_i} = (\Delta\varphi_{GX_i} \quad \Delta\varphi_{GY_i} \quad \Delta\varphi_{GZA_i} \quad \Delta\varphi_{GZB_i})^T$

angular increments w.r.t. an inertial frame per half second about the gyro input axes (arcsec per half second).

$\vec{N} = (N_{GX} \quad N_{GY} \quad N_{GZA} \quad N_{GZB})^T$

gyro outputs (arcsec per half second)

$\vec{SF} = (SF_{GX} \quad SF_{GY} \quad SF_{GZA} \quad SF_{GZB})^T$

gyro scalefactors (dimensionless)

$\vec{D} = (D_{GX} \quad D_{GY} \quad D_{GZA} \quad D_{GZB})^T$

gyro drifts (arcsec per half second)

For the angular increments per half second about the gyro input axes w.r.t. an inertial frame, the following function of the angular increments per half second about the axes of the control coordinate frame and the misalignments can be written:

$$\vec{\Delta\varphi}_{G_i} = \begin{pmatrix} GX_x & GX_y & GX_z \\ GY_x & GY_y & GY_z \\ GZA_x & GZA_y & GZA_z \\ GZB_x & GZB_y & GZB_z \end{pmatrix} * \begin{pmatrix} \Delta\varphi_{x_i} \\ \Delta\varphi_{y_i} \\ \Delta\varphi_{z_i} \end{pmatrix} = M * \vec{\Delta\varphi}_i \qquad (2)$$

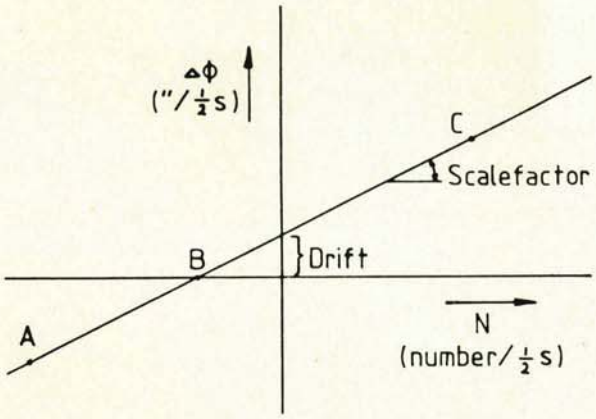

Figure 7. Gyro transfer function.

where:

GX_y is the projection of the unit vector along the GYRX input axis on the Y-axis of the control coordinate frame.

$\Delta\varphi_{x_i}$ is the angular increment per half second about the X-axis of the control coordinate frame.

M is the so-called misalignment matrix of the gyro input axes w.r.t. the control coordinate frame.

It will be assumed that the projection of the unit vector along a gyro input axis on the corresponding axis of the control coordinate frame is unity (cosine effect), thus

$$GX_x = GY_y = GZA_z = GZB_z = 1$$

Note that the misalignment matrix M is not an orthogonal matrix since the gyro input axes are not necessarily orthogonal.
In (2) it has been assumed that the angular increments per half second may be interpreted as velocities.
Combining (1) and (2) the following relation is obtained:

$$\vec{\Delta\varphi}_i = M^{-1} * \{ \vec{N} * \vec{SF} + \vec{D} \} \qquad (3)$$

which is implemented in the OBS to control the satellite on the basis of gyro outputs.

5. GYRO IN-FLIGHT TEST METHOD

The objective of the gyroscope in-orbit checkout is to establish the transfer function (scalefactor and drift) and the misalignments with respect to the control coordinate frame for each gyroscope, which then can be used in equation (3) on-board the satellite, and for reconstruction purposes on the ground.
The set of equations (3) shows 16 parameters to be solved during in-orbit checkout.

If an in-flight calibration manoeuvre is performed (3) gives a set of 4 equations with 16 unknowns. The gyro outputs N during the calibration manoeuvre are known from the telemetry and the inertial rotations about the control axes will be determined by means of two absolute sensors (FSS and SSE).
Sixteen equations with sixteen unknowns can be created by performing four independent different sorts of calibration manoeuvres from which the unknowns can be solved, assuming the scalefactor, drift and misalignment values remain constant.

The question now is: what kind of calibration manoeuvres must be performed in order to determine the requested parameters as accurately as possible.
Because of the non-linearity of the gyros and the fact that a linear transfer function is used, this linear function can be established with the best overall accuracy by determining a best fit straight line with measurements on many points at various angular rates. However, that will consume a lot of valuable flight time.
Another approach has been taken, based on the following types of observations, which are characteristic for the IRAS mission:

- survey scans (3.85 arcmin/sec)
- pointings
- low speed raster scans
- survey speed raster scans

Consider first the Z-axis gyros. Refering to the gyro transfer function in figure 7, survey scans would make use of point C on the transfer function, pointings employ point B, low speed raster scans are at speeds around point B and raster scans with survey speed are alternately at points A and C. It is essential to choose the calibration points on the transfer function at those angular rates about the GYRZ input axis that correspond to the velocities used in the high accuracy observation modes. Thereby the gyro transfer function is optimized for use at those angular velocities. In addition, the measurement time on each calibration point must be as long as possible in order to have minimum impact of SSE imperfections on the calibration accuracy. This rules out calibration point A for the Z-gyros due to attitude constraints imposed on IRAS. The remaining points B and C will be calibrated for the Z-axis gyros. Due to attitude constraints the satellite cannot rotate a complete orbit at survey speed. Point C will be at orbital speed, which is at 90% of the survey speed. During the routine phase statistical information of the transfer function will be built up using suitable survey scans. This information will be used to update the GYRZ transfer function every two weeks. This satisfies mostly the prime mission objective: the survey.

For the Y-axis gyro the important angular velocities (mainly during eclipses) are distributed over the velocity range of the gyro, with an emphasis on zero velocity (point B) since an observation scan is always performed with a constant solar aspect angle. For GYRY the transfer function will be calibrated at zero angular velocity and at plus and minus 12 arcmin/sec.

The input rates of the GYRX, which are important primarily during eclipse, will vary between $\pm$ 2.22 arcmin/sec. Again due to the attitude constraints it is not possible to accurately calibrate the transfer function at - 2.22 arcmin/sec. Consequently for GYRX, calibration points B and C will be established.
Summarizing, the following manoeuvres to calibrate the gyroscopes are selected:

- pointing
- Z-axis scan
- Y-axis scan (2 directions)
- X-axis scan

The complete calibration sequence as summarized here will be performed twice and the results of both tests will be compared for compatibility and ultimately be used for further refinement of the gyro transfer function calibration.

For each of those calibration manoeuvres it will now be discussed what the method is and whether special measures are prerequisite to reduce undesired pivot clearance and misalignment change effects.
Prior to and after each gyro calibration manoeuvre an attitude calibration with the SSE will take place on the basis of which the inertial rotations will be established.
In order to minimize systematic errors of the SSE and position errors of the used star while calibrating the gyros, the same bright star and the same most sensitive part of the SSE is employed for the preceding and following attitude calibration. These general guidelines will be followed for each calibration manoeuvre.

5.1. Pointing

A pointing in IRAS terminology means that the solar aspect angle θ and the angle about the sunvector ψ, which determine the satellite attitude with respect to the pseudo-inertial sun-referenced system (figure 4), remain constant. Note that this is not an inertial pointing since the earth, and thereby the sunvector, rotates about the sun. The use of a non-inertialized pointing eases the test evaluation on the ground. Prior to and after the pointing an attitude calibration will be performed with the SSE. These attitude calibrations will form the basis for the gyro transfer functions calibration at zero velocity. The inertial rotations between the two attitude calibrations will be established with the SSE and FSS.

Two independent pointings will be performed to improve knowledge on gyro characteristics by a factor of $\sqrt{2}$.

The duration of the pointing has to be taken as large as possible in order to maximize the accuracy of gyro calibration, however it is restricted to approximately 10 minutes to constrain the earth infrared radiation into the telescope. The change in thermal gradients during the pointings has to be limited in order to minimize the misalignment change between SSE and gyro package. This is achieved by scanning the satellite at the same solar aspect angle as the pointing for a complete orbit.

Concerning pivot clearance, with reference to section 3.3. it can be concluded that all gyros will show the same pivot behaviour namely a limit cycle centered on the preferred position, causing negligible gyro error outputs. The scan over a complete orbit prior to the pointing ensures that the pivots are indeed in their preferred positions at the start of the pointing.

5.2. Z-axis scan

A Z-axis scan is defined as a scan with a solar aspect angle of $\theta = 90°$ (refer to figure 4) with constant speed about the sunvector. The scan will be over 360° at orbital scan speed with attitude calibrations on the same star prior to and after the scan. Again these attitude calibrations are used as the basis for gyro calibration where the inertial rotations will be established with the SSE and FSS. The misalignment changes between SSE and gyros during the scan are minimized by starting the scan with thermal equilibrium, which is achieved by a complete orbit scan at a solar aspect angle of 90° prior to the Z-axis scan. As with the pointing, due to the limit cycle about the output axes of the gyros, pivot clearance effects hardly reduce the accuracy of this calibration.

5.3. Y-axis scan

A scan about the Y-axis can be obtained by keeping the angle about the sunvector ψ constant and changing the solar aspect angle (see figure 4) with a constant rate.
The Y-axis scan will start and end with an attitude calibration at a solar aspect angle of 60° and 120° respectively. The scanspeed will be 12°/min. This will be repeated in the reversed direction in order to improve the accuracy of transfer function determination.
To reduce the errors induced by misalignment changes between the SSE and the gyros the satellite will be brought to a thermal equilibrium at the same solar aspect angle as the start of the Y-axis scan. Since the time constant of the misalignment change is of the same order of magnitude as the duration of the manoeuvre the misalignment change will corrupt the Y-axis scan measurements.
By calibrating this misalignment change, one can eliminate related errors to a few arcseconds.

The pivot clearance effect drives to special measures in order to improve the accuracy of the gyro calibration. First consider the GYRX and GYRZA which have their output axes along the Y-axis. As discussed earlier the pivots of the gyros will limit cycle around the preferred positions at the end of the thermal stabilisation scan. During the Y-axis scan the pivots will move to the pivot restriction before the end of the Y-axis scan, causing an unknown gyro output error. This can be worked around by making an additional slew about the Y-axis of 2° with the same velocity sign as the Y-axis scan just after the thermal stabilization scan. This ensures the pivots to remain at one restriction throughout the manoeuvre.
Next consider the GYRY and GYRZB, which have their output axes along the satellite X-axis. During the attitude calibrations prior to and after the Y-axis scan the satellite will have an angular velocity about the X-axis.

By increasing this speed (making a short slew) the pivots will be forced to a pivot restriction prior to the attitude calibrations. Since the preceding and the following attitude calibrations have opposite X-axis velocity signs the Y and ZB gyro output has to be corrected for the pivot clearance amplitude which is known to an accuracy of approximately 3 arcsec.

5.4. X-axis scan

The IRAS cannot solely rotate about the X-axis since the Y-axis always remains perpendicular to the sunvector. The X-axis scan will be a scan about the sunvector with a solar aspect angle of $\theta = 60°$. From figure 4 it may be concluded that the velocities about the X- and Z-axes are coupled as follows:

$$\dot{\varphi}_x = -\dot{\varphi}_z \tan(\theta - 90°) = \dot{\psi} \cos\theta$$

The scan will cover 360° with attitude calibrations using the SSE at the beginning and end. The inertial rotations between the attitude calibrations will be established on the basis of SSE and FSS measurements. Thermal stabilisation to eliminate misalignment changes will take place at $\theta = 60°$.
Concerning pivot clearance the only difference with respect to the Z-axis scan is that the X-axis velocity drives the pivots of the GYRY and GYRZB towards the pivot restriction throughout the manoeuvre. Consequently pivot clearance induced errors are zero for these gyros.

6. TEST EVALUATION

The basis for the test evaluation will be
1° the inertial rotations as measured by the SSE and FSS
2° the gyroscope outputs
3° equation (3) which provides the relation between gyro output and inertial rotations.

The IRAS ground operations will provide the spacecraft engineers with telemetry data required for evaluation and perform bulk processing on e.g. the gyro outputs in such a way that the results can easily be interpreted and digested in the further evaluation. The results of the pre-processing on the four different calibration manoeuvres, two of which are performed twice, will lead to 24 equations with 16 unknowns (scalefactors, drifts and misalignments). Such an overdetermined set of equations can be solved conveniently with standard computer programs. If products of small terms are neglected in solving the unknowns, very simple equations result from (3) which can easily be evaluated by hand.

For the pointing for example the total inertial rotations are near zero, as well as the gyro misalignments. One can therefore safely assume that e.g. $GX_v * \Delta\varphi_{y_i} \ll \Delta\varphi_{x_i}$
The remaining equations from (3), which can be used for the pointing evaluation, are:

$$\vec{N} * \vec{SF} + \vec{D} = \vec{\Delta\varphi_i} \qquad (4)$$

If for evaluation of the Z-axis scan the same kind of approximations are employed, this will yield a similar equation for the Z-axis. Combining this with equation (4) the scalefactor and drift of the Z-gyros are solved.

Similarly the evaluation of the X-axis scan and the Y-axis scan will easily yield the transfer function of GYRX and GYRY.
The misalignments follow from the remaining equations (3).
Computer simulations will help to resolve whether the approximations approach is acceptable in view of the required accuracy.

For each gyro calibration manoeuvre as described in section 5 two reference times will be established, namely the start time and the end time corresponding to the very moments of the preceding and the following attitude calibration. For each manoeuvre the integrated gyro outputs between the reference times will be calculated and the inertial rotations between the reference times will be computed on the basis of SSE and FSS measurements. The latter measurements will be corrected for sun motion and limit cycle.

Since the satellite is controlled with respect to the non-inertial sun referenced system (figure 3) rotations with respect to this frame need to be translated into a rotation with respect to an inertial frame. This is obtained using the following relationship

$$\dot{\vec{\varphi}}_i = \dot{\vec{\varphi}}_s + \dot{\vec{\varphi}}_\odot \qquad (5)$$

where

$\dot{\vec{\varphi}}_i$ is the inertial angular velocity of the satellite
$\dot{\vec{\varphi}}_s$ is the satellite angular velocity w.r.t. the sun referenced frame
$\dot{\vec{\varphi}}_\odot$ is the inertial velocity of the sun referenced frame and equals the apparent angular velocity of the sun around the earth

Integration of equation (3) yields the desired inertial rotations of the satellite. From figure 4 it follows that the sun's velocity components along the satellite axes are:

$$\dot{\vec{\varphi}}_\odot = (\varphi_{\odot x} \;\; \varphi_{\odot y} \;\; \varphi_{\odot z})^T =$$

$$= \omega_\odot * (\cos\psi\sin\theta \;\; -\sin\psi \;\; -\cos\psi\cos\theta)^T \qquad (6)$$

Where $\omega_\odot$ is the sun's angular velocity
Since the sun motion has to be corrected for throughout the calibration manoeuvre, equation (6) has to be integrated from the start reference time to the end reference time:

$$\vec{\Delta\varphi}_\odot = \frac{\omega_\odot}{\Delta t} * \int \begin{pmatrix} \cos\psi \sin\theta \\ -\sin\psi \\ -\cos\psi \cos\theta \end{pmatrix} dt \qquad (7)$$

Where Δt is the time interval between the reference times. The sun's angular velocity is assumed constant during the test.
Integral (7) can be solved for each calibration manoeuvre separately. As an example the further groundprocessing method of the pointing will be discussed. In a similar way the other calibrations will be evaluated. For the pointing it is assumed that the angle about the sunvector is constant and corresponds to the mean angle about the sunvector of the calibration star at the start and the end reference times. Also the solar aspect angle is assumed constant during the test. The correction for the sunmotion from equation (7) then yields:

$$\vec{\Delta\varphi}_\odot = \omega_\odot * \begin{pmatrix} \cos\psi \sin\theta \\ -\sin\theta \\ -\cos\psi \cos\theta \end{pmatrix} \qquad (8)$$

The inertial rotation about the Z-axis between the reference times $\Delta\varphi_{Z_i}$ may be assumed to be zero. Integrating (5) and substituting (8), the inertial rotations per second become:

$$\begin{pmatrix} \Delta\varphi_{x_i} \\ \Delta\varphi_{y_i} \\ o \end{pmatrix} = \frac{1}{\Delta t} \int \dot{\vec{\varphi}}_s \, dt + \omega_\odot * \begin{pmatrix} \cos\psi \sin\theta \\ -\sin\theta \\ -\cos\psi \cos\theta \end{pmatrix} \qquad (9)$$

As may be concluded from figure 4 the velocities around the X and Z-axis during a scan about the sunvector are coupled as follows:

$$\dot{\varphi}_{X_s} = \dot{\varphi}_{Z_s} / \tan\theta \qquad (10)$$

With (10) substituted into the Z-equation of (9) the satellite angular rotation with respect to the sun referenced frame about the X-axis, $\Delta\varphi_{x_s}$ can be calculated:

$$\Delta\varphi_{X_s} = \frac{1}{\Delta t} \int \dot{\varphi}_{X_s} dt = \omega_\odot \cos\psi \cos\theta/\tan\theta \qquad (11)$$

Substitution of (11) into the X-equation of (9) yields the inertial rotation about the X-axis:

$$\Delta\varphi_{X_i} = \omega_\odot \cos\psi (\cos\theta/\tan\theta + \sin\theta) \qquad (12)$$

The inertial rotation about the Y-axis per second, using the same assumptions as before, becomes:

$$\Delta\varphi_{Y_i} = -\omega_\odot \sin\psi \qquad (13)$$

Note that the satellite angular rotation with respect to the sun referenced frame disappeared since the satellite is controlled with a constant solar aspect angle and "follows the sun".

As a next step the limit cycle at the two reference times will be corrected for the X- and Y-axes. For the Z-axis this is not required since the SSE directly provides the angle about that axis at the reference times.
Since the resolution of the gyros is a factor of 4 better than the resolution of the FSS, preferably the limit cycle must be reconstructed with the gyros. The gyro however, is not yet calibrated, so the output history of the relevant gyro is graphically overlayed with the output history of the FSS. The limit cycle amplitude at the reference time is then determined from the gyro output history by interpolation between two gyro measurements. The approach is depicted in figure 8. The drift related error in the gyro output cancels out using the overlaying technique, so the resulting error in limit cycle correction will correspond to the gyro scalefactor error, and will be fairly small since the limit cycle amplitude is less than 5 arcsec.

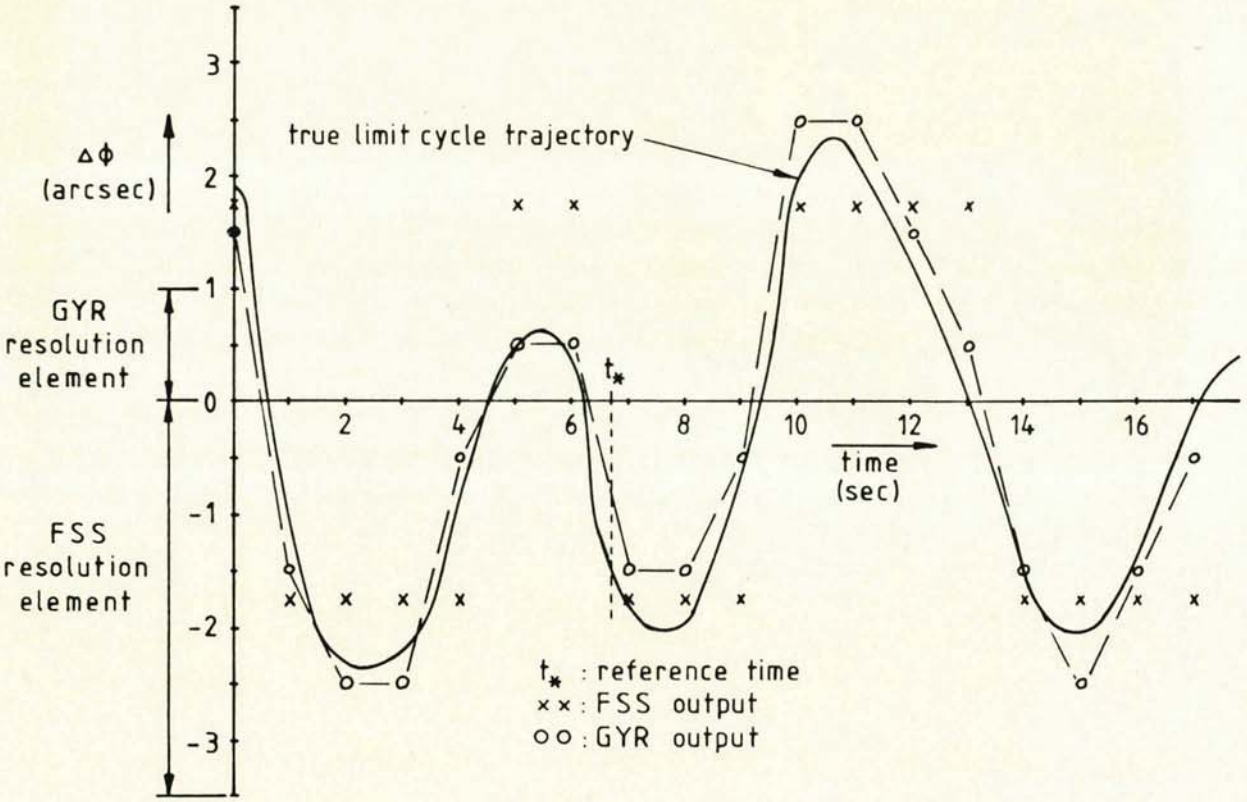

Figure 8 limit cycle reconstruction

Now the inertial rotations about the satellite axes per second over the calibration manoeuvre have been established, (for the Z-axis zero and for the X- and Y-axes in equations (12) and (13) corrected for limit cycle) these rotations are fed into equation (4), resulting in a set of expressions with two unknowns: scalefactors and drifts of all gyros. Similarly the groundevaluation on the other calibration manoeuvres will take place, each resulting in other sets of equations with unkowns from equation (3), which then can be solved.

7. CONCLUSION

The gyroscope is a prime sensor in the IRAS mission for both control and reconstruction of the telescope attitude. The high accuracy requirements impose a significant load on the method by which the gyroscopes will be calibrated in flight. It appears to be possible to meet those requirements if special calibration manoeuvres are designed such that the misalignment change effects due to thermal bending and gyro pivot clearance effects during the calibration manoeuvres are eliminated as far as feasible.
In addition the control and reconstruction accuracy of the primary observations modes, the survey scan, the low speed raster scan and the pointing, are increased by calibrating the gyro transfer function at the applicable angular velocities about the input axis.

8. REFERENCES

1. McLaughlin W.I., De Leeuw W.H.: "Infra-Red Astronomical Satellite" Spaceflight May p. 187-191 (1978)

2. Lundy S.A., McLaughlin W.I., Pouw A.: "Mission design for the Infra-Red Astronomical Satellite", 17th Aerospace Sciences meeting, New Orleans, January 15-17, AIAA-79-0125.

3. Van Bezooijen R.W.H.: "Iras Attitude Control Subsystem" Proc. of the ESA conference on "Attitude and Orbit Conbtrol Systems" Noordwijk, The Netherlands, October 3-6, p. 21-27 (1977)